DEFORMATION MECHANISMS IN A LAVES PHASE

Yaping Liu, Samuel M. Allen and James D. Livingson

Department of Materials Science and Engineering
Massachusetts Institute of Technology
Cambridge, MA 02139, USA

High Temperature Intermetallic Alloys-V Proceedings of Fall 1992
MRS Meeting, Boston, MA, accepted for publication. 11-30-92 to 12-3-92

ABSTRACT

The stress-induced phase transformation between C36 and C15 structures in Fe_2Zr is studied by electron microscopy. The nucleus of the transformation is believed to be some pre-existing C15 layers in C36 particles. Microstructural evidence for three mechanisms of growth of a new phase were found: Fault accumulation and rearrangement, moving of individual partial dislocations between two phases, and the migration of microscopic ledges composed of a series of Shockley partials between C36 and C15. Plastic deformation by slip on non-basal planes of C36 caused by indentation is studied.

I. INTRODUCTION

Stress-induced phase transformation has been found to be one of the martensitic transformation mechanisms in steels, many alloys and even semiconductors. However, there has been comparatively little work on this mechanism in Laves phases, probably due to the difficulty involved in the shear deformation in the phases of complex structure. Y. Ohba and N. Sakuma[1] observed a gum elastic deformation in $MgCu_2$ Laves phase when it was rapidly cooled from the melt, which was considered to be due to the stress-induced transformation, at a condition of very low stress and room temperature. Our previous work[2] used X-ray diffraction and electron microscopy to show that such a transformation could occur in a two-phase Fe-Zr alloy during uniaxial compression in room temperature. The present paper provides further results and discusses observations related to the nucleation and growth mechanism of the transformation in the Fe-10 at% Zr alloy.

Laves phases have three structure types: Cubic C15 ($MgCu_2$), hexagonal C14 ($MgZn_2$) or dihexagonal C36 ($MgNi_2$). The structure type appearing in a Laves phase is mainly determined by the electronic factor. Many studies suggested favorable ranges in terms of valence electron-to-atom ratios for the formation of Laves phases[3]. In Fe-Zr system, Kai et al.[4] found from their results of X-ray and magnetic measurements that two single-phase regions of dihexagonal ($MgNi_2$-type) and of cubic ($MgCu_2$) Laves phase are located in two separate composition ranges from 27.3 to 31.4 at% Zr and from 32.8 to 34.0 at% Zr, respectively. Because of the eutectic point at 8.8 at% Zr, The 10 at% Zr alloy used in the present study contains substantial amounts of both eutectic and pro-eutectic Fe_2Zr Laves phases.

II. EXPERIMENTAL

The Fe-10 at% Zr alloy used in the study was prepared by arc melting. Samples for compression testing were then cut from the arc-cast ingots using an electric-discharge machine. The size of the samples was 5×5×5 mm. Samples were encapsulated in a vacuum of 10^{-6} Torr and annealed at 1190°C for 48 hours. Compression experiments were performed at room temperature with a crosshead speed of 2.5×10^{-3} cm/min. Indentations were performed at room temperature in a DM 400 Microhardness Tester, and 10 × 10 arrays of 50 g Vickers indentations were made on the central part of alloy disks which are 3 mm in diameter and 300 μm in thickness.

TEM specimens approximately 0.4 mm thick were cut from the undeformed and compressed samples using a diamond saw, ground to a thickness of 0.1 mm, and electropolished in a solution of 10% perchloric acid-90% methanol. Ion milling was also used in some samples to get addional thin area for high resolution microscopy. The indentation samples were polished and dimpled to 30 μm followed by atom-mill

FG02-90ER45426

thinning to electron transparency. A JEOL 200CX and an Akashi EM-002B high-resolution transmission electron microscope operating at an accelerating voltage of 200 kV were used in the microstructure analysis. A Vg HB5 scanning transmission electron microscope with a minimum probe size of 0.5 nm was used in the compositional micro-analysis. The thin sections cut from undeformed and compressed samples were also used in X-ray diffraction experiments, which were performed on an RIGAKU RU300 diffractometer with Cu-K_α radiation and a rotating anode. In order to minimize the influence of any possible texture produced by the compression, X-ray specimens were cut at random orientations from lateral faces of the compressed samples.

III. RESULTS AND DISCUSSION

A typical nominal stress-strain curve is shown in Fig.1. Samples of the annealed alloy were deformed in compression at room temperature to strains of 46-48% without any macroscopic cracks or load drops. The 0.2% offset yield strength $\sigma_{0.2}$ of the alloy is about 730 MPa. Microstructural analysis by TEM revealed that the α-Fe matrix was heavily deformed, as it contained a high density of dislocation arrays, networks and tangles. On the other hand, SEM revealed many cracks in the pro-eutectic Laves particles. The chemical compositions of both the eutectic and pro-eutectic Fe_2Zr were determined to be in the range of 29-30 at% Zr, by STEM composition micro-analysis.

X-ray diffraction provided evidence that microstructure changes had occurred within the Laves phase. Comparison of the X-ray diffraction pattern of samples before and after compression in Fig.2 shows that the dominant structure of the Laves phase in undeformed samples is C36. However, after deformation, the intensity of peaks of C15 increased. Repeated experiments on many samples showed the same result: the volume fraction of C15 structure increased after compression. To study the detail and mechanism of the phase transformation, the microstructures of both compressed and undeformed alloys were observed using TEM. Transmission electron microscopy revealed extensive faulting in the C36 Laves phase before deformation. A high-resolution lattice image is shown in Fig.3, in which the stacking sequence of close-packed planes is indicated by the line superimposed on the figure. The typical dihexagonal C36 structure is a mixture composing a half hexagonal (h) and a half cubic (c) components, with a stacking sequence of "hchc". The existence of the faults changes the stacking sequence of some of the layers in the figure, as indicated by the arrows. Closer examination of the faults reveals that they can be divided into two types. In the first type two or more (but usually no more than 7-8) cubic type layers stack continuously, changing the stacking sequence into, say, "hcchc" as indicated by arrow A in the figure. This can be interpreted as an insertion of a "c" layer or a removal of a "h" layer. The second type is a continuous stacking of "h" layers, but

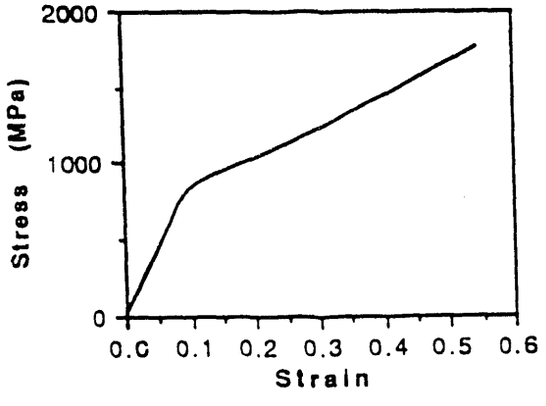

Fig.1 Stress-strain curve of room temperature compression test of Fe-10 at% Zr alloy.

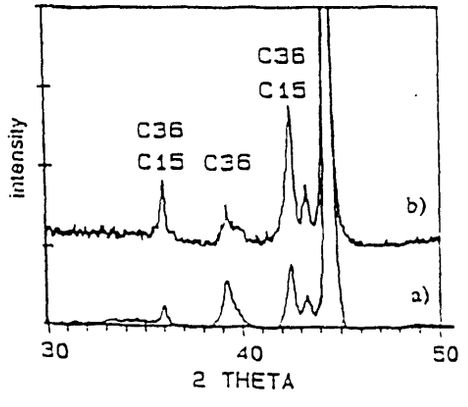

Fig.2 X-ray diffraction patterns of (a) undeformed and (b) compressed alloy.

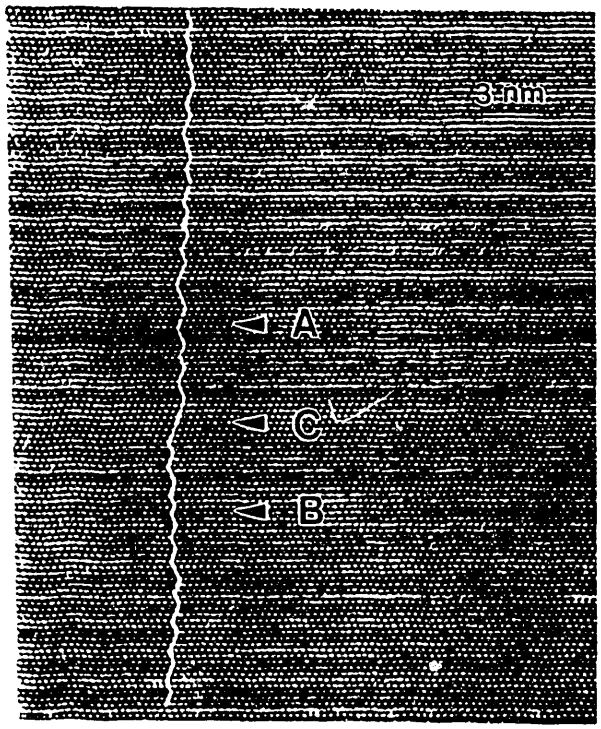

Fig.3 Stacking sequence of undeformed C36 planes showing the faults (A and B) and a nucleus of C15 structure (C).

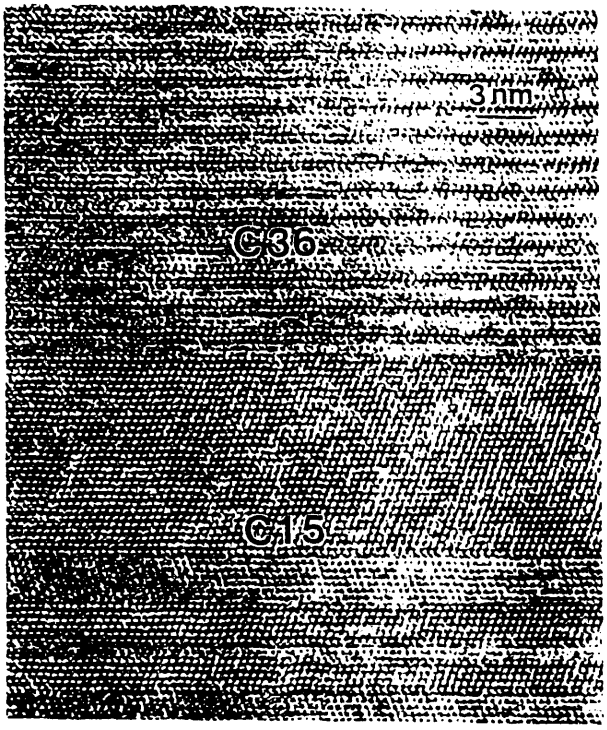

Fig.4 New phase C15 formed in a C36 particle caused by the compression.

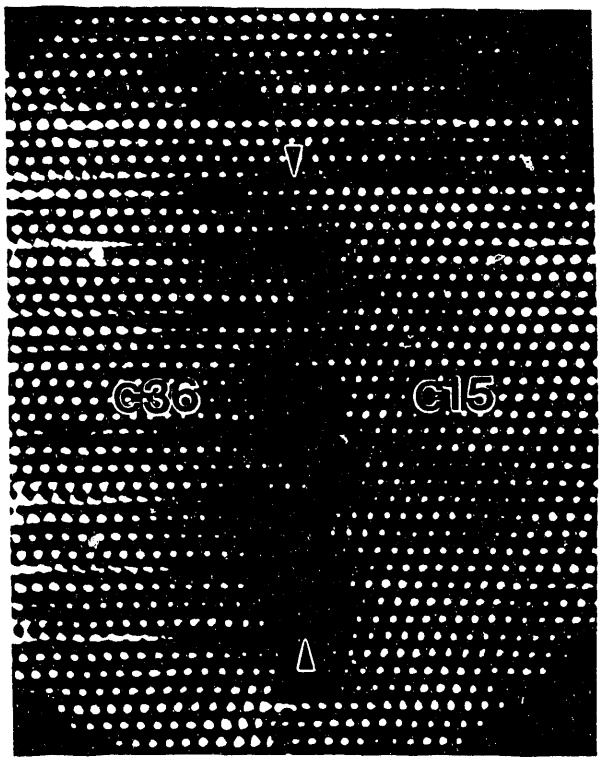

Fig.5 Computer enhanced picture of ledge interface between C15 and C36.

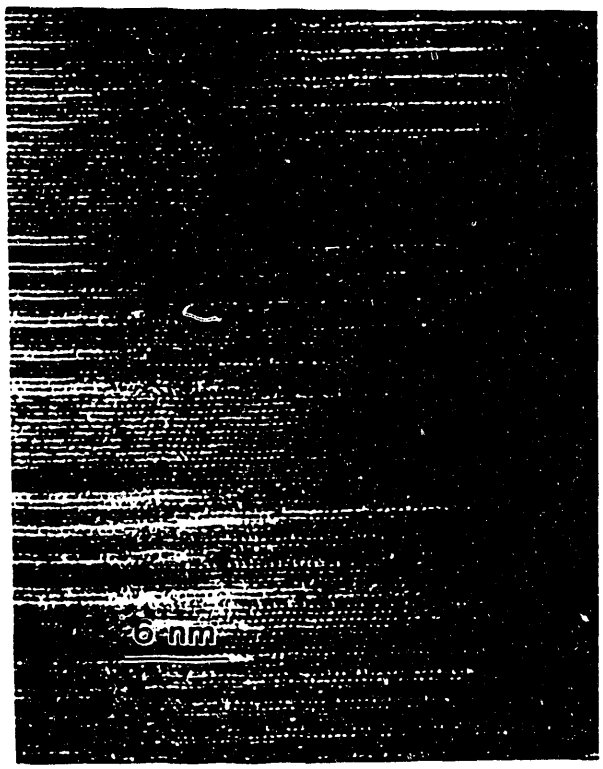

Fig.6 Growth mechanism: Gathering of faults and narrow C15 bands near a C15 nucleus.

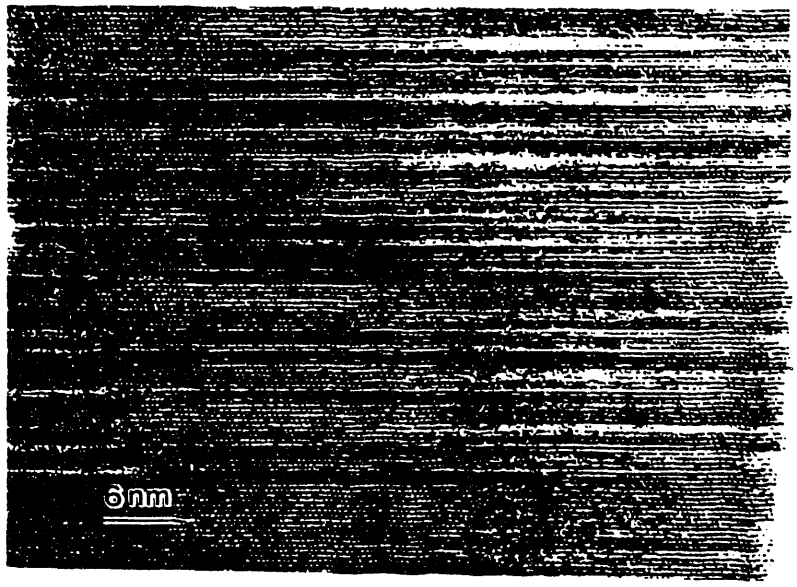

Fig 7 Growth mechanism: Moving of single partials between two phases.
To the left , There are more and more C15; to the right, more and more C36.

usaully no more than two layers, as indicated by arrow B in the figure. This is a insertion of a "h" layer or a removal of a "c" layer. The first type is more common than the second one, causing the composition of the mixture to deviate from the ideal 50% hexagonal and 50% cubic components. Statistical calculation on many micrographs shows the mixture is: 54% cubic and 46% hexagonal stacking componants.

The high density of stacking faults implies a low stacking fault energy and hence easy nucleation and growth of a new phase. It should be noted that the continuous stacking of "c" layers, indicated by C in Fig.3, is frequently observed in the alloy. The pre-existing C15 layers should be the nuclei for the phase transformation. It is interesting that the layer numbers of the C15 nuclei in many particles are almost all the same (7-8 layers).

After compression, the new phase C15 was found in the Laves particles by electron microscope in a band morphology. An example is shown in Fig.4. Looking along the zone axis of $[2\bar{1}\,\bar{1}0]_{C36}/[011]_{C15}$ in the figure one can easily distinguish between the C15 area which has nearly pure "c" stacking, and the C36 area which has the stacking sequence "hchc".

The phase transformation between C36 and C15 is a shear transformation, which occurs by the glide of Shockley partial dislocations of Burgers vector b = a/6 <211> [5,6] and involves two partials every four layers[2]. By observing and analyzing numerous pictures of Laves particles containing both C15 and C36 structures, some mechanisms of growth of a new phase are suggested: Firstly, the transformation proceeds gradually from one narrow band to another adjacent band, by the motion of an interface with microscopic ledges composed of a series of Shockley partials between C36 and C15. This interface can be observed in a computer enhanced TEM picture in Fig.5, indicated by two arrows. The locations of the partial dislocations are also marked in the figure. This mechanism has been discussed in detail in [2].

Besides the migration of the ledge interface, the new phase can grow by a widening mechanism. This was frequently observed on dark-field images, which showed the contrast of high density faults and narrow C15 bands gathering near the C15 area. Faults may increase in density due to the stress concentration near the nucleus in the compression, and some of the faults may rearrange to a periodic sequence in which there are two faults every four layers. These rearranged layers thus become some narrow C15 bands, which have lower energy. An example is shown in Fig.6. These

faults and narrow bands may extend into a large region of the new phase. In this mechanism, the growth direction is normal to the coherent interface between C36 and C15:

Fig.7 shows the third mechanism of growth of the new phase. In the figure, C36 and C15 are located at right and left ends along the "basal planes", respectively. They are seperated by a "transition area" which consists of a series stacking faults and partial dislocations. In the area close to the right, the stacking is more like C36; to the left, more like C15. In this case, the new phase can grow by means of the moving of single partial dislocations. Then the single C15 components in the transtion area grow normal to the basal plane, and the large C15 area grows parallel to the basal plane to the right to extend the new phase area.

Microhardness testing showed that the hardness of the alloy was 350 HV. The diagonal length and the depth of the indents were 16.9 μm and 2.4 μm, respectively. No crack was found at corners or other areas of the any of the indents, indicating a considerable toughness value of the two-phase alloy. Other than twinning and faults on C15 area and transformation in C36 area caused by compression[2], the indentation can produce other types of deformation. Low magnification TEM pictures revealed a large shear strain occuring on non-basal planes of the lamellar Laves phase. These shears are approximately normal to basal plane. The distance between two single shears is typically several hundred angstroms. This can be seen in Fig.8. High-resolution TEM pictures, such as Fig.9, show that the slips may not be restricted on a certain plane, and the shear distance may vary from 1 basal plane thickness to more than ten basal planes. These can be shown by the slip line on the left and that on the right in Fig.9, respectively. Comparison of the Lamellar structure at different areas shows that the shears usually occur within 20 μm from the indents, and can not be found at the areas further away. This confirms the shears are caused by the indentation. This type of deformation needs further study.

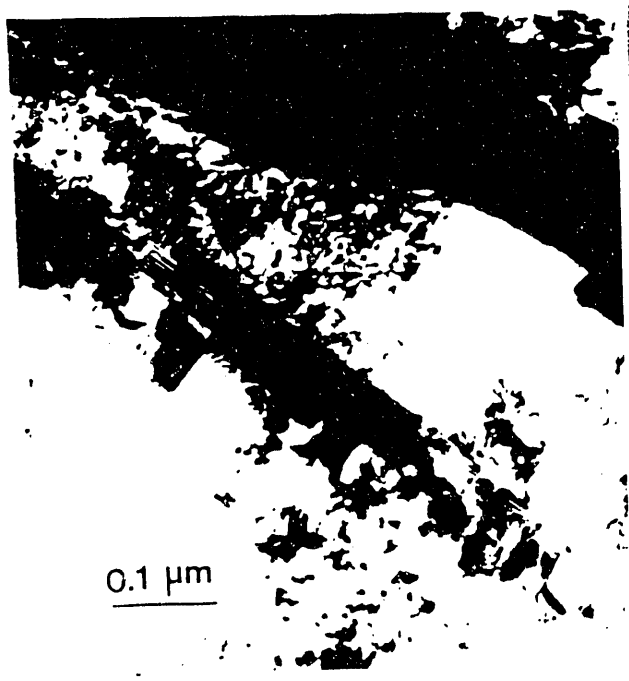

Fig.8 Slips on lamellar C36 caused by indentation. Slip planes are normal to basal plane.

Fig.9 High-resolution TEM picture of slips on C36 caused by indentation, showing the slip distance varying from one to more than ten basal panes.

IV. SUMMARY

Nucleus for the phase transformation from C36 to C15 was found to be the pre-existing C15 thin layers which may cause a stress concentration near the interface. Besides the microscopic ledge interface migration mechanism, the new phase can grow normal to the coherent interface by creating faults to widen the C15 band, or grow along basal plane by the moving of some individual dislocations to lengthen the new phase. Non-basal plane shear slip was found to be another form of deformation caused by indentation. The slip planes are aproximately normal to basal plane.

ACKNOWLEDGEMENT

Financial support from the Department of Energy, Division of Basic Energy Sciences, Grant No. DE-FG02-90ER45426, is greatly appreciated. We also acknowledge the helpful discussions with Kathy Chen and the providing of computer enhancement of TEM micrographs by Ernest L. Hall.

REFERENCES

[1] Y. Ohba and N. Sakuma, Acta Metall., Vol. 37, No. 9, 2377, (1989).

[2] Yaping Liu, James D. Livingston, and Samuel M. Allen, Met. Trans. A, Vol. 23A, No 12, (1992).

[3] J. H. Westbrook, Intermetallic Compounds, Robert E. Krieger Publishing Company, 1977.

[4] K. Kai, T. Nakamichi and M. Yamamoto, J. Phys. Soc. Japan, Vol. 25, 1192, (1968).

[5] C. W. Allen and K. C. Liao, Phys. Stat. Sol. (a) 673-681, 74, (1982).

[6] C. W. Allen, H. R. Kolar and J. C. H. Spence, Proceedings of The International Conference on Martensitic Transformations, The Japan Institute of Metals, Sendai, Japan, 1986, p. 186-191.

[7] G. B. Olson and M. Cohen, Ann. Rev. Mater. Sci., 11:1-30, (1981).

[8] J. D. Livingston, Phys. Stat. Sol.(a) 131, 415, (1992).

[9] J. D. Livingston and E. L. Hall, J. Mater. Res., Jan., Vol. 5, No. 1, 5-8, (1990).

END

DATE
FILMED
10/5/93